

Saturation Self-Organizing Map

Igor Urbanik^{1*} and Paweł Gajewski¹

^{1*}Faculty of Computer Science, AGH University of Krakow, al. Adama Mickiewicza 30, Kraków, 30-059, Poland.

*Corresponding author(s). E-mail(s): igorurbanik23@gmail.com;
Contributing authors: pgajewski@agh.edu.pl;

Abstract

Continual learning poses a fundamental challenge for neural systems, which often suffer from catastrophic forgetting when exposed to sequential tasks. Self-Organizing Maps (SOMs), despite their interpretability and efficiency, are not immune to this issue. In this paper, we introduce Saturation Self-Organizing Maps (SatSOM)—an extension of SOMs designed to improve knowledge retention in continual learning scenarios. SatSOM incorporates a novel saturation mechanism that gradually reduces the learning rate and neighborhood radius of neurons as they accumulate information. This effectively freezes well-trained neurons and redirects learning to underutilized areas of the map.

We evaluate SatSOM on sequential versions of the FashionMNIST and KMNIST datasets and show that it significantly improves knowledge retention compared to usual methods, while approaching the performance of the memory-intensive k-nearest neighbors (kNN) baseline. Ablation studies confirm the critical role of the saturation mechanism. SatSOM offers a lightweight, interpretable, and memory-efficient approach to sequential learning and lays the groundwork for extending adaptive plasticity to broader neural architectures.

Keywords: Continual Learning, Self-Organizing Map, Catastrophic Forgetting, Knowledge Retention, Sequential Learning

1 Introduction

Intelligent agents navigating real-world environments must continuously learn, adapting to new information while retaining prior knowledge [Parisi et al. \(2019\)](#). This ability, known as continual or lifelong learning, poses a significant challenge in modern machine learning. Most artificial neural systems struggle with catastrophic forgetting [French](#)

(1999), where training on new tasks or data distributions abruptly erases previously learned information.

This phenomenon stems from the shared nature of representations in standard neural networks, where updating weights for new data can overwrite information critical for past tasks. Overcoming catastrophic forgetting is crucial for developing robust, adaptable systems that can learn incrementally from data streams, rather than being retrained from scratch.

Numerous approaches have been proposed to mitigate catastrophic forgetting, ranging from regularization techniques and memory replay to architectural modifications. However, many state-of-the-art solutions, despite showing promising results, require substantial changes to model structure or training procedures. This often limits their compatibility with widely used and well-understood machine learning frameworks. Notable exceptions, such as Elastic Weight Consolidation (EWC) [Kirkpatrick et al. \(2017\)](#), retain compatibility with standard architectures by selectively preserving parameters deemed important for previous tasks. Nevertheless, in our experiments, EWC still exhibits significant forgetting, especially when compared to a simple baseline: the k-nearest neighbors (kNN) algorithm.

kNN serves as a strong reference point in continual learning research because it stores all training data and simply compares new inputs to this memory during inference, avoiding forgetting by design. However, this strength is also its main drawback: it is not a feasible solution for real-world continual learning scenarios due to its unbounded memory requirements and lack of generalization.

In this work, we address the challenge of enhancing knowledge retention in neural networks while directing learning signals to underutilized model components, a critical issue in continual learning. We propose a novel extension to the Self-Organizing Map (SOM) [Kohonen \(1982\)](#), called Saturation Self-Organizing Map (SatSOM), which introduces a saturation mechanism to preserve learned representations and improve learning efficiency in dynamic environments. Self-Organizing Maps are shallow, unsupervised learning models that organize high-dimensional data into a low-dimensional, typically two-dimensional, grid, making them easy to visualize and interpret. By leveraging a distance-based metric, SOMs cluster data points based on similarity, akin to the k-Nearest Neighbors (kNN) algorithm. While kNN achieves near-perfect retention by design, but its reliance on distance metrics and unbounded memory makes it impractical for large-scale or real-time applications. Similarly, SOMs, despite their simplicity and interpretability, are constrained in model capacity compared to modern deep learning architectures. Nevertheless, their structured representation of data makes them an ideal testbed for exploring knowledge retention strategies.

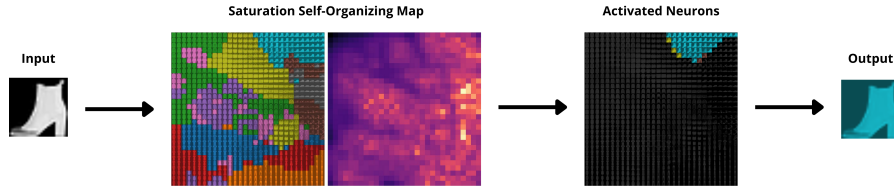


Fig. 1 Symbolic visualization of SatSOM inference on the FashionMNIST dataset.

Our SatSOM architecture builds upon prior efforts to enhance SOMs for continual learning, such as those explored in the PROPRES framework [Gepperth and Karaoguz \(2017\)](#), which aimed to make SOMs knowledge-retaining. SatSOM introduces a novel saturation metric, distinct from traditional neuron saturation concepts in neural networks. This metric quantifies the amount of data a neuron has absorbed, reflecting its learning capacity. Once a neuron reaches a predefined saturation threshold, further weight updates are restricted, preserving critical learned patterns while allowing less-utilized neurons to continue adapting. This mechanism mitigates catastrophic forgetting, a prevalent challenge in continuous learning, by balancing stability and plasticity in the model. See Figure 1 for a broad overview of our method.

The significance of SatSOM lies in its ability to significantly improve knowledge retention in SOMs, as demonstrated through our experiments. By preventing overfitting to new data and preserving previously learned representations, SatSOM enhances the robustness of SOMs in continual learning scenarios. Furthermore, the principles underlying the saturation mechanism offer promising insights for improving knowledge retention in other neural architectures, potentially extending its impact beyond SOMs to more complex models.

This work showcases SatSOM as a practical and interpretable solution for continual learning, leveraging the simplicity of SOMs to explore advanced learning dynamics. Our findings suggest that the saturation metric could serve as a foundational concept for designing more resilient and adaptive neural networks, opening new avenues for research in continual learning and knowledge retention.

All the model architecture and testing code related to this article is available in a GitHub repository¹.

2 Related Work

A comprehensive survey found in [Delange et al. \(2021\)](#) provides a detailed overview of continual learning methods, highlighting the ongoing challenge of evaluating them effectively. In this section we will highlight the three main schools of thought present in literature.

The first, regularization-based methods, focus on constraining the updates of neural network weights during the learning of new tasks to protect knowledge from previous tasks. The primary example from this school is Elastic Weight Consolidation (EWC) proposed by [Kirkpatrick et al. \(2017\)](#). It addresses catastrophic forgetting by remembering old tasks by selectively slowing down learning on the weights important for those tasks. It achieves this by adding a quadratic penalty to the loss function which constrains important parameters to stay close to their old values. The importance of each parameter is estimated using the diagonal of the Fisher information matrix.

Rehearsal-based methods, also known as replay- or exemplar-based methods, prevent catastrophic forgetting by storing a subset of data from past tasks and mixing them with data from the current task during training. One such method is iCaRL (incremental classifier and representation learning), introduced by [Rebuffi et al. \(2017\)](#),

¹<https://github.com/Radinyn/satsom>

a strategy to simultaneously learn classifiers and a feature representation in a class-incremental setting. A key feature of iCaRL is its use of a fixed-size set of exemplars to represent past classes. These exemplars are chosen via a herding-based method and used for a nearest-mean-of-exemplars classification rule. The framework uses both the exemplars for rehearsal and a distillation loss to update the feature representation without forgetting. Another memory-efficient replay-based approach was proposed by [Hayes et al. \(2019\)](#).

The final school, architectural and hybrid methods, includes all (but is not limited to) the adaptations of the SOM architecture for continual learning. Other researchers have proposed several architectural modifications:

[Gepperth and Karaoguz \(2017\)](#) showcased that SOMs can achieve near-state-of-the-art performance on certain continual learning tasks. This is the primary paper that inspired our work. There are also other energy-based Self-Organizing Map training methods proposed by the same first author (e.g. [Gepperth \(2017\)](#)).

SOMPL proposed by [Bashivan et al. \(2019\)](#) combines a standard supervised network with a SOM layer that runs in parallel. The SOM’s role is to cluster inputs into task contexts and create an output mask, which selectively routes the input to the most relevant parts of the network without requiring explicit task labels.

DendSOM proposed by [Pinitas et al. \(2021\)](#) draws inspiration from biological dendrites, this architecture uses a single layer composed of multiple SOMs, where each SOM acts like a dendrite modeling a specific subregion (or receptive field) of the input space. It also proposes using cosine similarity for BMU selection as an alternative to Euclidean distance.

The Continual SOM (CSOM) introduced by [Vaidya et al. \(2024\)](#) is a generalization designed for online, task-free learning. Its key innovations include embedding each neuron with its own running variance and, similarly to SatSOM neuron-specific learning parameters (learning rate and neighborhood radius). We were not aware of that model’s existence during our testing, because of their similarity, we would like to highlight the novelty of our work:

- Unlike CSOM, SatSOM does not maintain running variance, but achieves comparable performance regardless using simple euclidean distance.
- SatSOM uses a quantile threshold parameter to select only the relevant neurons, stabilizing the results.
- The simpler structure of SatSOM allows us to perform a complex ablation study and identify key future research directions that may include adapting the saturation concept to different machine learning models.
- In this paper we introduce the comparison to a kNN model, showcasing it’s superiority over both approaches on a benchmark.

3 Methodology

3.1 Saturation Mechanism

The *Saturation Self-Organizing Map (SatSOM)* is based on the idea that we can preserve information by forcing new knowledge to be learned in parts of a model that do not currently play important roles in the prediction. This is further reinforced and made easier by SOM’s intuitive grid structure.

This idea is realized by giving each neuron its own learning rate and neighborhood radius that decays over training based on the magnitude of changes that were applied to it, effectively freezing them after a certain threshold. In this paper, we call the difference between the initial learning rate and the current learning rate *saturation*, although it could be just as well defined on the basis of the neighborhood radius.

SatSOM works by learning a set of prototypes (grid points, neuron weights) and label-prototypes. Each time a prediction is made the model matches the input with most similar prototypes based on a predefined (here: Euclidean) distance function and returns a weighted output based on their respective label-prototypes. It can be easily visualized as shown in Figure 2.

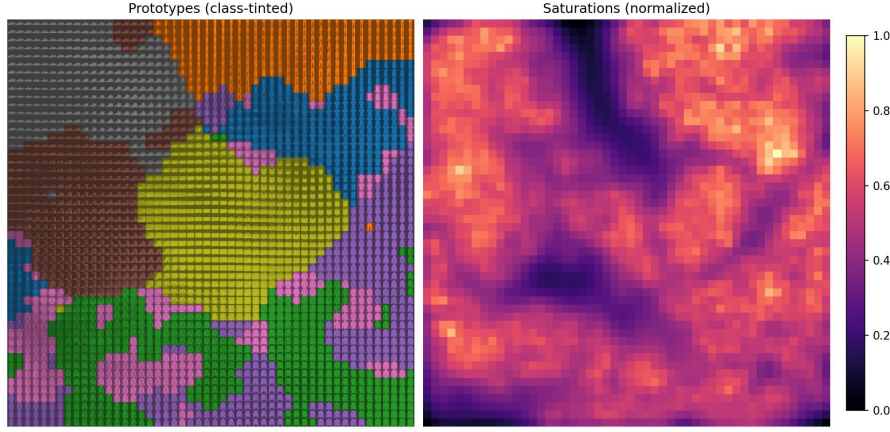


Fig. 2 This is an example visualization on a SatSOM trained to classify the FashionMNIST dataset. The prototypes are visualized as little images that are later compared with the new input to perform classification. They have been tinted based on the class that has the highest probability in their respected label-prototype.

Our intuition is that the neighborhood radius decay guides new knowledge to the emptier parts of the map, while preserving the locality of changes. In contrast, learning rate decay works by preserving the more important neurons when no more space can be found. This view is further reinforced by the results of our ablation study (see Section 5).

3.2 Definitions

First, we define all the dimensions:

$$\begin{aligned}
dim_M &\in \mathbb{N} && \text{(number of grid dimensions, here 2)} \\
dim_I &\in \mathbb{N} && \text{(input dimensions)} \\
dim_O &\in \mathbb{N} && \text{(output dimensions, number of classes)} \\
n &\in \mathbb{N} && \text{(size of the grid)} \\
N &= n^{\dim_m} && \text{(number of neurons)}
\end{aligned}$$

The model can be mathematically interpreted as the following variable quantities:

$$\begin{aligned}
W &\in \mathbb{R}^{N \times \dim_i} && \text{(prototype weight matrix)} \\
w_j &\in \mathbb{R}^{\dim_i} && \text{(row } j \text{ of } W) \\
L &\in \mathbb{R}^{N \times \dim_o} && \text{(label-prototype matrix)} \\
\ell_j &\in \mathbb{R}^{\dim_o} && \text{(row } j \text{ of } L) \\
\Lambda &= (\lambda_1, \dots, \lambda_N)^\top && \text{(learning rate vector)} \\
\Sigma &= (\sigma_1, \dots, \sigma_N)^\top && \text{(neighborhood radius vector)}
\end{aligned}$$

And one constant matrix:

$$\begin{aligned}
G &\in \mathbb{R}^{N \times \dim_m} && \text{(grid coordinate matrix)} \\
G &= \{0, \dots, n-1\}^{\dim_M} && \text{(cartesian product)} \\
g_j &\in \mathbb{R}^{\dim_m} && \text{(row } j \text{ of } G)
\end{aligned}$$

The model parameters change based on the following hyperparameters:

$$\begin{aligned}
\lambda_0 &\in \mathbb{R} && \text{(initial learning rate, used to initialize } \Lambda) \\
\sigma_0 &\in \mathbb{R} && \text{(initial neighborhood radius, used to initialize } \Sigma) \\
\alpha_\lambda &\in \mathbb{R} && \text{(learning rate decay)} \\
\alpha_\sigma &\in \mathbb{R} && \text{(neighborhood radius decay)} \\
\alpha_{bias} &\in \mathbb{R} && \text{(additional bias for undersaturated neurons)}
\end{aligned}$$

There are also inference-time hyperparameters:

$$\begin{aligned}
q &\in (0, 1) && \text{(neuron activation quantile threshold)} \\
p &\in \mathbb{R} && \text{(distant neuron penalty)}
\end{aligned}$$

Although SatSOM has many hyperparameters, in this paper we show that specific combinations of those parameters are effective for most tasks.

We also define saturation of a neuron as:

$$s_i = \frac{\lambda_0 - \lambda_i}{\lambda_0}, \quad i = 1, \dots, N. \quad (1)$$

3.3 Training

The training procedure begins by presenting a single example x together with its one-hot-encoded label y . First, the Best-Matching Unit (BMU) is found by computing Euclidean distances

$$d_i = \|x - w_i\|_2, \quad (2)$$

and selecting its index:

$$b = \arg \min_i d_i. \quad (3)$$

Around this BMU, each neuron i acquires a neighborhood strength:

$$\theta_i = \exp\left(-\frac{\|g_i - g_b\|^2}{2\sigma_b \sigma_i}\right). \quad (4)$$

This neighborhood strength can be further modified by the saturation. In further testing this step did not bring a meaningful improvement to the accuracy, but we decided to keep it for clarity:

$$\theta_i \leftarrow \theta_i (1 + \alpha_{bias}(1 - s_i)). \quad (5)$$

Each prototype w_i is then nudged toward the sample by

$$w_i \leftarrow w_i + \lambda_i \theta_i (x - w_i). \quad (6)$$

Concurrently, the label matrix is updated by first calculating the class probabilities (softmax)

$$p_{i,c} = \frac{\exp(\ell_{i,c})}{\sum_{c'} \exp(\ell_{i,c'})}, \quad (7)$$

computing the gradient $\nabla \ell_i = p_i - \ell$, and applying

$$\ell_i \leftarrow \ell_i - \lambda_i \theta_i \nabla \ell_i. \quad (8)$$

Afterwards, both the per-neuron learning rate and radius decay multiplicatively according to the neighborhood strength:

$$\lambda_i \leftarrow \lambda_i \exp(-\alpha_\lambda \theta_i), \quad \sigma_i \leftarrow \sigma_i \exp(-\alpha_\sigma \theta_i). \quad (9)$$

3.4 Inference

The model makes a prediction by creating a weighted average of select label-prototypes. A symbolic visualization is shown in Figure 1.

We start with normalizing the distance ($\varepsilon > 0$):

$$\tilde{d}_i = \frac{d_i - \min_j d_j}{\max_j d_j - \min_j d_j + \varepsilon}. \quad (10)$$

Next we disable under-saturated neurons:

$$\tilde{d}_i \leftarrow 1 \quad \text{if} \quad s_i < \varepsilon \quad (11)$$

We compute the cut-off quantile threshold on enabled neurons

$$\tau = \text{quantile} \left(\{ \tilde{d}_j : \lambda_j \geq \varepsilon \}, q \right), \quad (12)$$

and clamp any \tilde{d}_i exceeding τ to unity:

$$\tilde{d}_i \leftarrow 1 \quad \text{if} \quad \tilde{d}_i > \tau. \quad (13)$$

Finally, distances are converted into neuron *proximities* via the exponent (p), sharpening the fall-off:

$$h_i = \left(1 - \tilde{d}_i \right)^p. \quad (14)$$

We use the label matrix to compute the final prediction, weighted by proximity:

$$\hat{y} = \frac{1}{N} \sum_{i=1}^N h_i \ell_i \in \mathbb{R}^{\text{dim}_O}. \quad (15)$$

4 Experimental Evaluation

We decided to benchmark SatSOM and other architectures on a fairly extreme knowledge retention test. The model was tasked with classifying two 10-class datasets, FashionMNIST [Xiao et al. \(2017\)](#) and KuzushijiMNIST [Clanuwat et al. \(2018\)](#) (KMNIST), with a 70-30 train-validation split. The training was divided into phases. A single phase consisted of training on one and only one entire class. After each phase, the model classified the entire validation set. Each experiment was run 10 times to make sure the results are reproducible.

Apart from a kNN ($k = 5$) we compared SatSOM to some usual neural networks. These models were reinforced with *Online Elastic Weight Consolidation (OnlineEWC)*, a mechanism proposed by [Kirkpatrick et al. \(2017\)](#) and later modified into its online version by [Schwarz et al. \(2018\)](#). It is meant to preserve important weights by penalizing their change based on their individual Fisher Information gathered during training. For training, we used the Adam optimizer.

The exact neural networks reinforced with OnlineEWC were:

1. A multilayer perceptron (MLP) with two hidden layers of sizes 400 and 200, each using ReLU activation.
2. A convolutional neural network (CNN) consisting of:

- Two convolutional layers with 32 and 64 filters respectively, each with a kernel size of 3;
- Each convolutional layer is followed by a ReLU activation and max pooling;
- A fully connected head with two layers, the first having 128 hidden units.

It should be noted that neural networks very often require multiple passes of data to achieve desired results. To accommodate for that, each of the previously mentioned models was trained on 10 epochs of each class. We also show their results when they were trained on only one. Both SatSOM and kNN were trained in a single pass.

The hyperparameters used in this experiment are shown in table 1. Both the SatSOM and OnlineEWC hyperparameters were significantly tuned to prepare for that task. It should be noted that, although unusual, we did not find any meaningfully different hyperparameter sets for OnlineEWC that yielded results distinguishable from random choice.

Table 1 Hyperparameters used in the test

kNN	SatSOM	OnlineEWC	Value
k	—	—	5
—	n	—	100
—	λ_0	—	0.5
—	σ_0	—	10
—	α_λ	—	0.01
—	α_σ	—	0.2
—	α_{bias}	—	0.9
—	p	—	10
—	q	—	0.001
—	—	OnlineEWC α	$1 - 10^{-5}$
—	—	OnlineEWC λ	10^8
—	—	Adam α	10^{-8}
—	—	Adam β_1	0.9
—	—	Adam β_2	0.999

The results are shown and are further described in the figures: 3, 4, 5, 6.

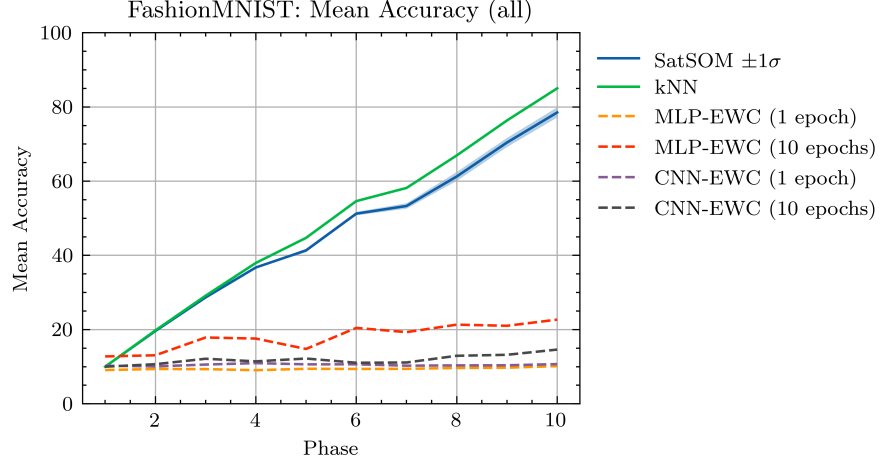


Fig. 3 Mean accuracy on all FashionMNIST classes through the 10 phases. SatSOM memory retention is comparable to that of the kNN. OnlineEWC results do not surpass the 30% threshold.

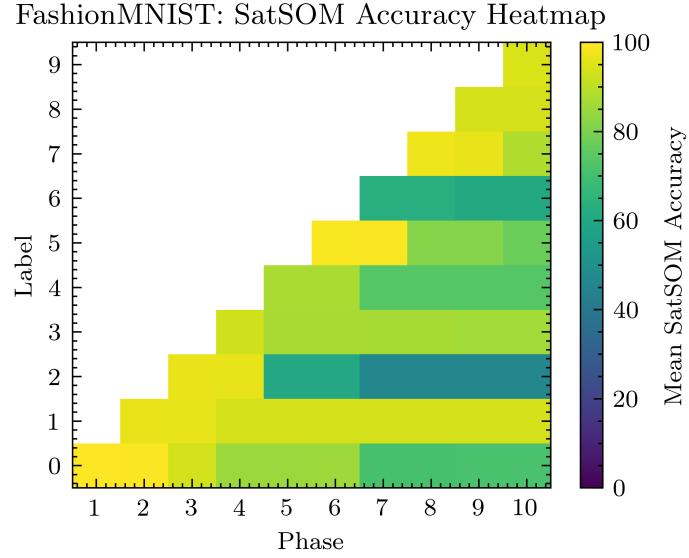


Fig. 4 Heatmap of mean SatSOM accuracy (FashionMNIST) on each class.

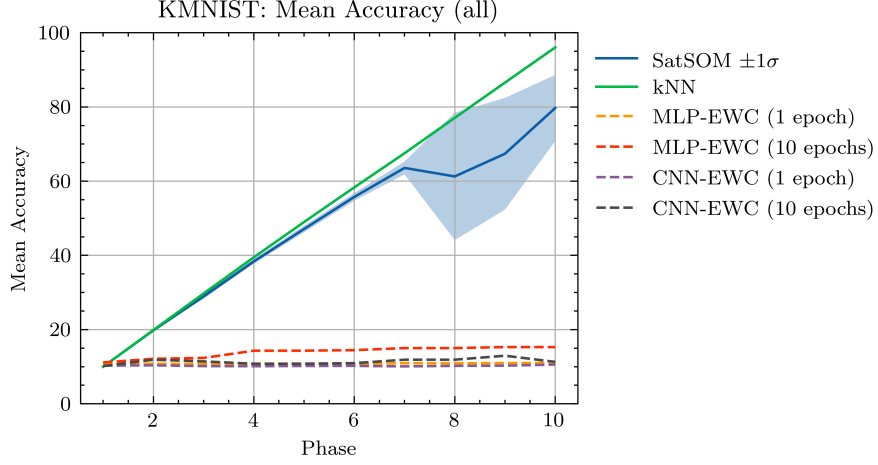


Fig. 5 Mean accuracy on all KMNIST classes through the 10 phases. There is a significant increase in standard standard deviation after the introduction class 8.

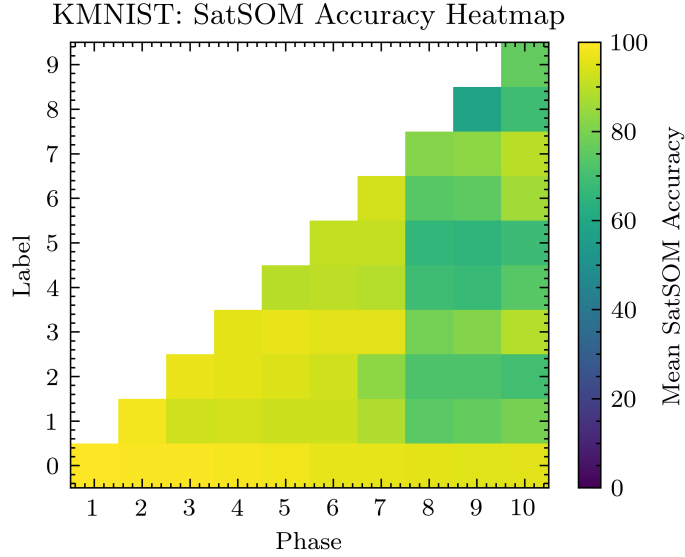


Fig. 6 Heatmap of mean SatSOM accuracy (KMNIST) on each class. There is a noticeable loss of accuracy after the introduction of class 8. It is likely happening due to its visual similarity to other classes.

SatSOM shows significant, kNN-like long-term memory, showcasing its potential. OnlineEWC models even after extensive hyperparameter tuning do not achieve comparable results, although it must be admitted that this scenario is not realistic and is merely a scientific tool for measuring knowledge retention.

The model also does not require any human input prior to the introduction of a new class, making it versatile in real-world scenarios.

A step by step visualization of a SatSOM training during one of the KMNIST runs is shown in figures 7 (prototypes) and 8 (saturation). The general low saturation of the network (relative to Figure 2) is due to the choice of hyperparameters.

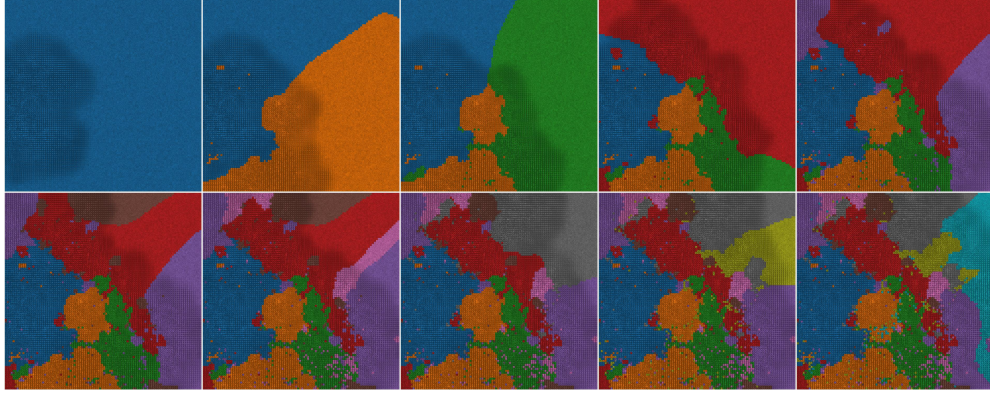


Fig. 7 Prototypes through a single training on the KMNIST dataset (left to right, top to bottom).

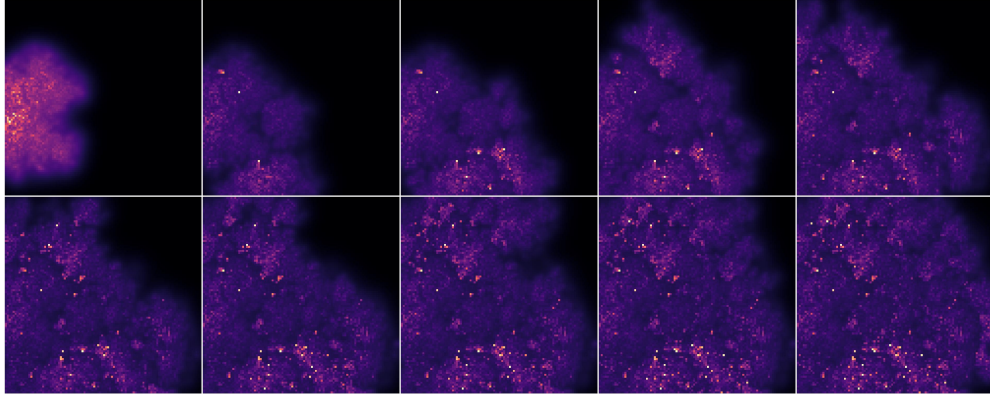


Fig. 8 Saturation through a single training on the KMNIST dataset (the same as in Figure 7).

5 Ablation Study

To measure the impact of the most important algorithm elements we decided to repeat the same test as in Section 4, this time inhibiting select hyperparameters. All other hyperparameters were set to the exact values as seen in table 1. The dataset used was FashionMNIST. All runs were repeated 10 times.

5.1 Learning Rate Decay

Inhibition of α_λ by setting it to zero required additional change to avoid the quantile threshold disabling all the neurons (see Equation 12). For this test we temporarily re-defined saturation (see Equation 1) on the basis of Σ instead of Λ :

$$s_i = \frac{\sigma_0 - \sigma_i}{\sigma_0}, \quad i = 1, \dots, N. \quad (16)$$

We also ran this test for two map sizes, the common $n = 100$ (Figure 9) and memory constrained $n = 20$ (Figure 10). The purpose of this is to show the situation in which learning rate decay comes into play.

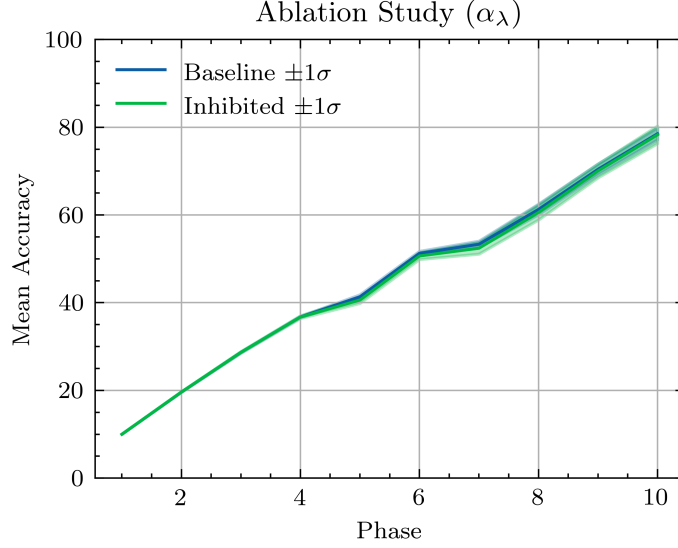


Fig. 9 Mean SatSOM accuracy (FashionMNIST) comparison between the base model and the inhibited model with $\alpha_\lambda = 0$. The plot shows no impact due to the model’s effectively unconstrained memory ($n = 100$).

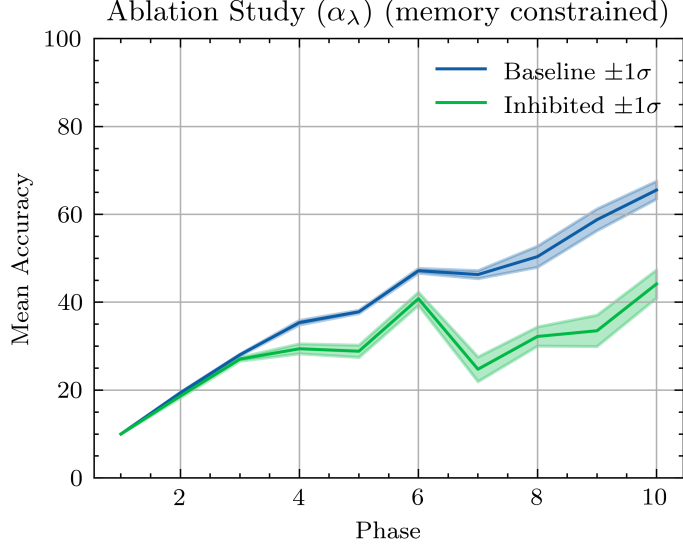


Fig. 10 Mean SatSOM accuracy (FashionMNIST) comparison between the base model and the inhibited model with $\alpha_\lambda = 0$ in a memory constrained environment ($n = 20$). The effect of α_λ is clearly visible.

The effect of α_λ is noticeable only in the $n = 20$ example. This behavior showcases α_λ as an important hyperparameter preventing knowledge loss in memory constrained environments and reinforces α_σ as the main factor when SatSOM is not yet over-learned.

5.2 Neighborhood Radius Decay

In the next test, we set α_σ to 0. Although the model demonstrates some knowledge retention, it quickly loses its ability to learn new classes (Figure 11). The ones on which the model was already trained already occupy too much of the map (see Figure 12). This also shows that SatSOM’s memory is strictly limited by the choice of n .

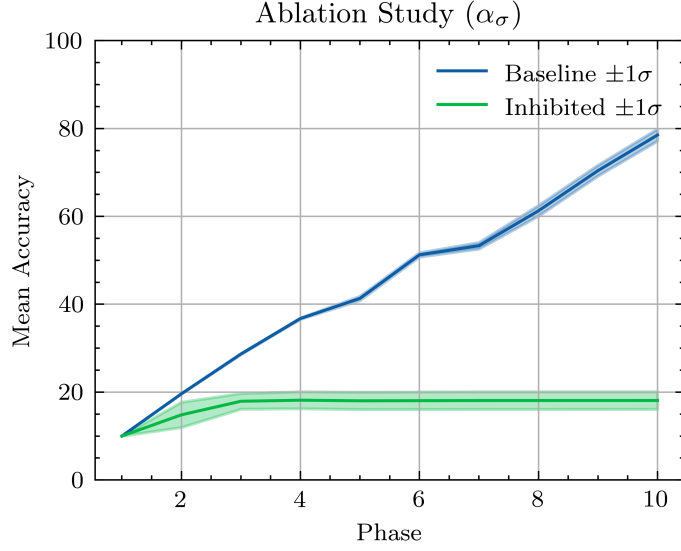


Fig. 11 Mean SatSOM accuracy (FashionMNIST) comparison between the base model and the inhibited model with $\alpha_\sigma = 0$. There is a visible cut-off of accuracy in the inhibited model.

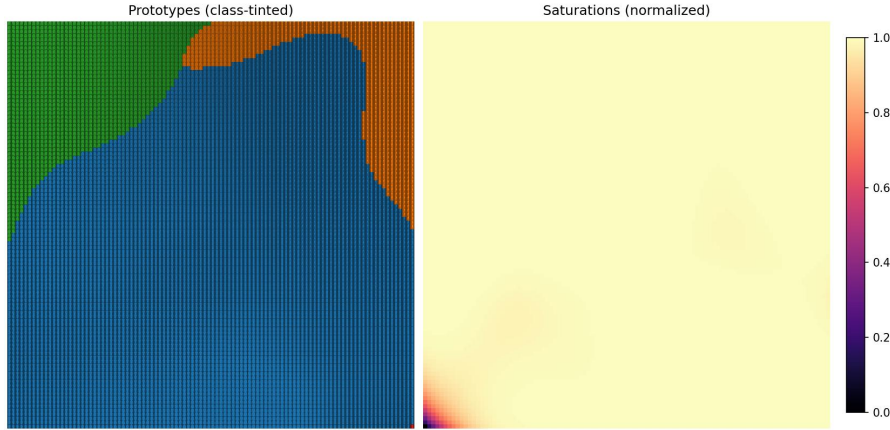


Fig. 12 Example SatSOM after 10 phases with inhibited neighborhood radius decay. Only 3 classes are present.

5.3 Additional Bias

As previously mentioned, zeroing bias appears to have no significant effect on the model (Figure 13). We decided to leave it in the paper for the sake of future research.

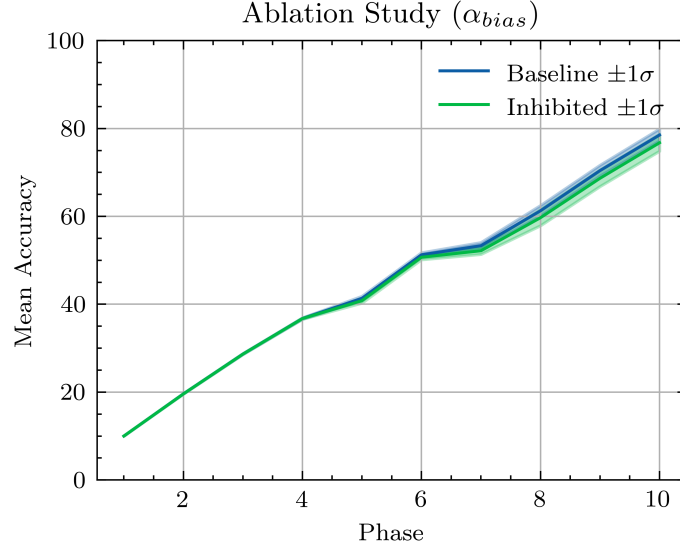


Fig. 13 Mean SatSOM accuracy (FashionMNIST) comparison between the base model and the inhibited model with $\alpha_{bias} = 0$. There is no visible difference.

5.4 Quantile Threshold

Inhibiting q by setting it to 1 diminishes the model performance by including many irrelevant neurons in the final label calculation (Figure 14). SatSOM output becomes more sensitive to class sizes, as their relative size on the map weighs on the output, increasing the standard deviation.

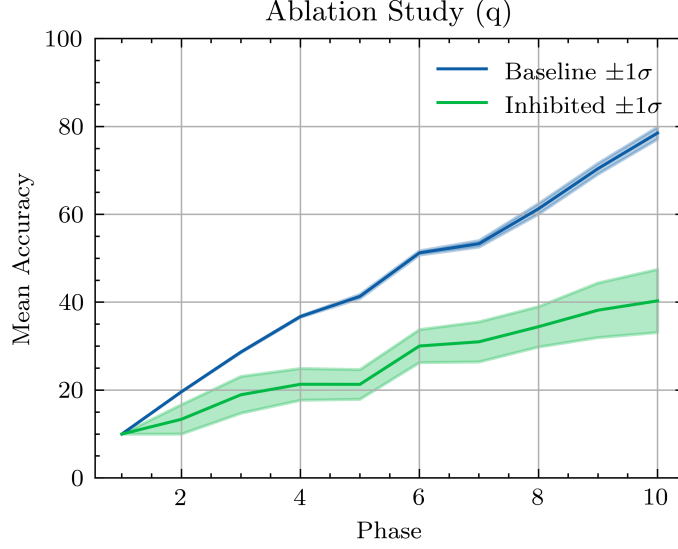


Fig. 14 Mean SatSOM accuracy (FashionMNIST) comparison between the base model and the inhibited model with $q = 1$. The base model achieved superior results in all the runs.

6 Hyperparameter Analysis

We would also like to showcase a basic hyperparameter grid search that we performed during the initial prototyping along with additional insights and intuitions. The exact grid parameters are found in table 2.

Table 2 Hyperparameter search values

Parameter	Values
n	50, 100
λ_0	0.5
σ_0	$\frac{n}{2}$
α_λ	0.01
α_σ	10^{-3} , 10^{-2} , 10^{-1} , 1
α_{bias}	0, 0.2, 0.5, 1
p	10
q	10^{-5} , 10^{-4} , 10^{-3} , 10^{-2}

This time, the test consisted of two phases, as shown in table 3, and was run on both previously mentioned datasets. SatSOM was trained 10 times for each hyperparameter set. All of the results were later aggregated. Because some obviously bad combinations existed within the grid the model accuracy and standard deviation is subpar.

Table 3 Classes used in the test

Phase 1	Phase 2
0, 1, 2, 4, 5, 6, 7, 8	3, 9

As shown in Figure 15, and according to all our other tests, the grid size (n) has no observable effect on the model accuracy as long as it is large enough. It is, as expected, a primary determinant of the model’s maximum capacity.

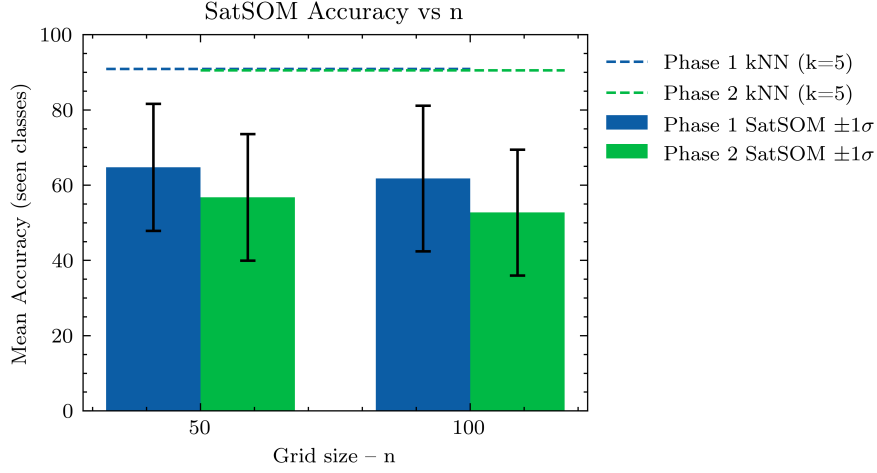


Fig. 15 Mean SatSOM accuracy in regards to the n hyperparameter. There is no clear difference between the two values.

We found that neighborhood radius decay (α_σ) between 0.01 and 0.1 is suitable for most applications (Figure 16). Values outside of that range tend to produce unstable results or be clearly ineffective.

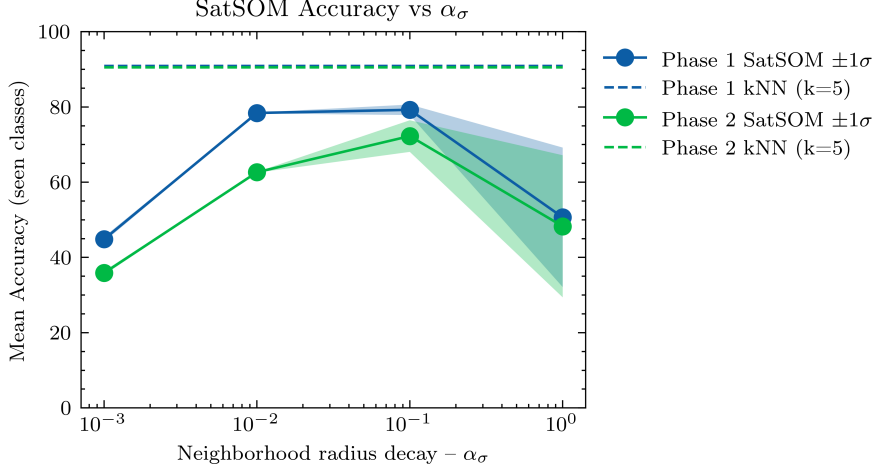


Fig. 16 Mean SatSOM accuracy in regards to the α_σ hyperparameter. Values near the beginning of the range produce unsatisfactory results, while higher values have a high standard deviation.

As shown in Figure 17, most values of the quantile threshold (q) worked relatively well, with a slight advantage on values closer to 0.01.

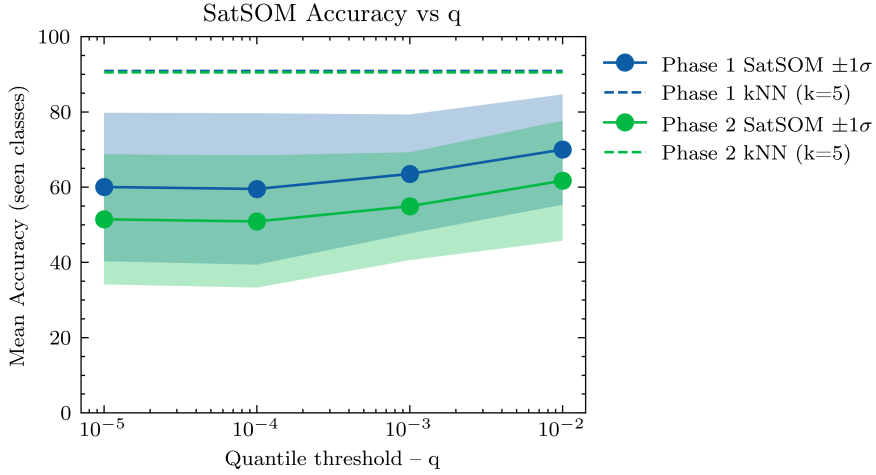


Fig. 17 Mean SatSOM accuracy in regards to the q hyperparameter. All the values within the range produce satisfactory results.

Although we do not have formal evidence, our empirical observations during testing suggest that reducing the initial neighborhood radius (σ_0) improves knowledge retention, albeit at the cost of requiring more input data. In contrast, increasing σ_0

accelerates training, but tends to reduce knowledge retention. Based on these findings, we recommend using a lower value of σ_0 when retention is a priority. Typically $\sigma_0 = \frac{n}{2}$ is used as a starting point.

7 Conclusion & Future Work

In this paper, we introduced SatSOM, a novel extension of the SOM algorithm designed to enhance knowledge retention in continual learning scenarios. The key innovation of SatSOM is a saturation mechanism, which modulates the learning rate and neighborhood radius based on a neuron’s training history. As a neuron accumulates knowledge, its capacity for further updates diminishes, effectively freezing its weights. This dynamic encourages the acquisition of new information by neurons that remain unsaturated, thereby minimizing the risk of overwriting previously learned representations.

Our empirical results demonstrate that SatSOM significantly improves performance in continual learning tasks. It clearly outperforms OnlineEWC, a widely used regularization-based approach, and approaches the performance of kNN, despite not storing any past data. Importantly, ablation studies confirm that the saturation mechanism is the primary contributor to these improvements, underscoring its value in managing learning dynamics over time.

This research contributes to the broader effort of developing continual learning systems that are efficient, stable, and compatible with existing machine learning methods. Most state-of-the-art approaches to catastrophic forgetting require substantial modifications to model architecture or training protocols, limiting their applicability. In contrast, SatSOM offers a lightweight, interpretable alternative that avoids external memory, explicit task boundaries, or rehearsal, making it especially promising for resource-constrained applications.

Looking ahead, several directions emerge from this work. One avenue is the adaptation of the saturation principle to deep neural networks, potentially through layer-wise or neuron-specific plasticity control, which could enable similar preservation of learned features. Another promising direction is the development of hierarchical or stacked SatSOM architectures, which could capture increasingly abstract representations while maintaining continual learning capabilities at each level. SatSOM might also be integrated into hybrid systems, serving as a stable feature extractor within larger learning pipelines or as a guide for generative replay. Moreover, due to its simplicity and independence from stored data, SatSOM is well suited for on-device learning in embedded systems, robotics, and other environments with limited computational resources.

In summary, SatSOM offers a biologically inspired and computationally efficient approach to continual learning, demonstrating that adaptive modulation of plasticity can play a critical role in mitigating catastrophic forgetting. This work lays the groundwork for extending these principles to more complex architectures and broader applications.

8 Acknowledgements

We thank Dr. Leszek Grzanka for his support in running the experiments.

This research was supported by the funds assigned to AGH University by the Polish Ministry of Education and Science.

9 Compliance with Ethical Standards

This research adheres to all applicable ethical standards and guidelines. All datasets used in this work are publicly available and widely used in the research community for benchmarking machine learning models. The authors declare that they have no conflict of interest.

References

- Bashivan P, Schrimpf M, Ajemian R, et al (2019) Continual learning with self-organizing maps. URL <https://arxiv.org/abs/1904.09330>, arXiv:1904.09330
- Clanuwat T, Bober-Irizar M, Kitamoto A, et al (2018) Deep learning for classical japanese literature. <https://doi.org/10.20676/00000341>, URL <http://arxiv.org/abs/1812.01718>, cite arxiv:1812.01718Comment: To appear at Neural Information Processing Systems 2018 Workshop on Machine Learning for Creativity and Design
- Delange M, Aljundi R, Masana M, et al (2021) A continual learning survey: Defying forgetting in classification tasks. *IEEE Transactions on Pattern Analysis and Machine Intelligence* PP:1–1. <https://doi.org/10.1109/TPAMI.2021.3057446>
- French RM (1999) Catastrophic forgetting in connectionist networks. *Trends in cognitive sciences* 3(4):128–135
- Gepperth A (2017) An energy-based som model not requiring periodic boundary conditions. In: 2017 12th International Workshop on Self-Organizing Maps and Learning Vector Quantization, Clustering and Data Visualization (WSOM), pp 1–6, <https://doi.org/10.1109/WSOM.2017.8020018>
- Gepperth A, Karaoguz C (2017) Incremental learning with self-organizing maps. In: 2017 12th International Workshop on Self-Organizing Maps and Learning Vector Quantization, Clustering and Data Visualization (WSOM), IEEE, pp 1–8
- Hayes TL, Cahill ND, Kanan C (2019) Memory efficient experience replay for streaming learning. In: 2019 International Conference on Robotics and Automation (ICRA). IEEE Press, p 9769–9776, <https://doi.org/10.1109/ICRA.2019.8793982>, URL <https://doi.org/10.1109/ICRA.2019.8793982>
- Kirkpatrick J, Pascanu R, Rabinowitz N, et al (2017) Overcoming catastrophic forgetting in neural networks. *Proceedings of the National Academy of Sciences* 114(13):3521–3526. <https://doi.org/10.1073/pnas.1611835114>, URL <https://www.pnas.org/doi/abs/10.1073/pnas.1611835114>, <https://www.pnas.org/doi/pdf/10.1073/pnas.1611835114>

- Kohonen T (1982) Self-organized formation of topologically correct feature maps. *Biological cybernetics* 43(1):59–69
- Parisi GI, Kemker R, Part JL, et al (2019) Continual lifelong learning with neural networks: A review. *Neural networks* 113:54–71
- Pinitas K, Chavlis S, Poirazi P (2021) Dendritic self-organizing maps for continual learning. URL <https://arxiv.org/abs/2110.13611>, [arXiv:2110.13611](https://arxiv.org/abs/2110.13611)
- Rebuffi SA, Kolesnikov A, Sperl G, et al (2017) icarl: Incremental classifier and representation learning. In: 2017 IEEE Conference on Computer Vision and Pattern Recognition (CVPR), pp 5533–5542, <https://doi.org/10.1109/CVPR.2017.587>
- Schwarz J, Czarnecki W, Luketina J, et al (2018) Progress & compress: A scalable framework for continual learning. In: International conference on machine learning, PMLR, pp 4528–4537
- Vaidya H, Desell T, Mali A, et al (2024) Neuro-mimetic task-free unsupervised online learning with continual self-organizing maps. URL <https://arxiv.org/abs/2402.12465>, [arXiv:2402.12465](https://arxiv.org/abs/2402.12465)
- Xiao H, Rasul K, Vollgraf R (2017) Fashion-MNIST: a Novel Image Dataset for Benchmarking Machine Learning Algorithms. *arXiv e-prints* arXiv:1708.07747. <https://doi.org/10.48550/arXiv.1708.07747>, [arXiv:1708.07747](https://doi.org/10.48550/arXiv.1708.07747) [cs.LG]